Water Resources Research

RESEARCH ARTICLE
10.1029/2022WR032670

Partitioned Soil Water Balance and Its Link With Water Uptake Strategy Under Apple Trees in the Loess-Covered Region

Peijun Shi[1], Haoqi Gai[1], and Zhi Li[1]

[1]State Key Laboratory of Soil Erosion and Dryland Farming on the Loess Plateau, College of Natural Resources and Environment, Northwest A&F University, Yangling, China

Key Points:

- Stable and radioactive water isotopes were combined to partition soil water balance (SWB) and quantify land use change impacts
- Apple tree planting increases transpiration by decreasing soil water storage and deep drainage
- Changes in SWB are closely related to the mining of deep soil water by apple trees

Supporting Information:

Supporting Information may be found in the online version of this article.

Correspondence to:

Z. Li,
lizhibox@nwafu.edu.cn

Citation:

Shi, P., Gai, H., & Li, Z. (2023). Partitioned soil water balance and its link with water uptake strategy under apple trees in the Loess-covered region. *Water Resources Research*, *59*, e2022WR032670. https://doi.org/10.1029/2022WR032670

Received 24 APR 2022
Accepted 16 DEC 2022

Author Contributions:

Conceptualization: Zhi Li
Formal analysis: Peijun Shi
Funding acquisition: Zhi Li
Investigation: Peijun Shi, Haoqi Gai
Methodology: Peijun Shi, Zhi Li
Project Administration: Zhi Li
Supervision: Zhi Li
Visualization: Peijun Shi
Writing – original draft: Peijun Shi, Haoqi Gai
Writing – review & editing: Zhi Li

Abstract It is important, but challenging, to partition soil water balance (SWB) to understand the impacts of afforestation on soil hydrological processes. This study will investigate the partitioning of SWB by combining stable and radioactive water isotopes to quantify the effects of afforestation, and analyze the mechanism by which SWB changes through identifying the water uptake strategies of apple trees of 18 and 26 years old (A18 and A26). Compared to the reference farmland, apple orchards significantly increased evapotranspiration (ET) by 5%–10%, which in turn decreased soil water storage and deep drainage by 5%–14% and 50%–95%, respectively. Further, the partitioning of ET showed that apple tree planting increased transpiration by 15%–28% but decreased evaporation by 17%–30%. The above change in SWB appeared to be closely related to plant water uptake strategies. The apple trees shifted their water source from shallow (0–2 m) to deep soils (below 2 m), utilizing approximately 62% of deep soil water in the late growing season. In particular, 23% of source water may come from soil water older than 50 years. The older apple trees tended to extract more water from deeper soils (45% for A26 vs. 38% for A18). Therefore, the soil water deficit was the cumulative effects of root water uptake. The methods for SWB partitioning provides technical support for similar studies, and the findings are helpful to better understand the hydrological processes in the thick loess deposition.

1. Introduction

Vegetation, as an important medium connecting atmosphere and landscape (Jasechko et al., 2013), plays a leading role in linking water, energy, and carbon cycle (Bastin et al., 2019). Over the past decades, to combat global warming and land degradation, global vegetation has witnessed tremendous changes (Bryan et al., 2018; Tong et al., 2018), resulting from the Restoration Initiative in Asia, the Great Green Wall of Africa, and the Grain for Green Project in China (Chen et al., 2019; Liu et al., 2008). In particular, growing interest in afforestation projects will be more popular to achieve the Paris Agreement climate goal (Bastin et al., 2019; Duan et al., 2021; Zhang et al., 2022). Although the benefits of afforestation have been recognized globally (Doelman et al., 2020; Duan et al., 2021; Hermoso et al., 2021), the sustainability of revegetation is often questioned (Feng et al., 2016; Holl & Brancalion, 2020). Therefore, it is imperative to understand the relationship between afforestation and hydrological variability to promote their harmonious coexistence.

As a main component of global terrestrial freshwater, the water stored in soils is crucial for vegetation growth (Evaristo et al., 2015; Li et al., 2017; Wang et al., 2018). Soil water availability may determine the growth of vegetation in dry regions. In turn, the plants can influence different components of SWB (e.g., evaporation *E*, transpiration *T*, and deep drainage *D*) through various water use strategies (Good et al., 2015; Knighton et al., 2019; Zhang & Wei, 2021). Previous studies have indicated that afforestation could lead to growth in *ET* (Jaramillo et al., 2018; Shi, Huang, Ji, et al., 2021; Wang, Cheng, et al., 2021), decreases in surface runoff and soil water storage (Luo et al., 2020; Scott & Lesch, 1997; Sun et al., 2006; Zhang, Yang, et al., 2018), and perturb the hydraulic connectivity in dry regions (Han et al., 2020; Shi, Huang, Yang, & Li, 2021). However, most studies focus on a specific SWB component, and have not systematically evaluated the impacts of afforestation on SWB. Therefore, it is urgent to investigate how each component of SWB changes after tree planting and the mechanism behind the changes.

It is necessary to do the partitioning of SWB under different plants to decipher plant-water interaction. Both hydrological modeling and isotope-based methods are commonly employed techniques for this purpose (Kool

et al., 2014; Sun et al., 2021). In particular, with the development of isotope measurement technology, the isotope-based techniques have been widely used to investigate ecohydrological processes (Evaristo et al., 2015; Good et al., 2014; Jasechko et al., 2013). As an effective strategy to estimate evaporation loss and identify water uptake strategies of plants (Evaristo et al., 2015; Gessler et al., 2021; Good et al., 2014; Sun et al., 2021), stable isotopes ($\delta^{18}O$, $\delta^{2}H$) can't partition SWB without additional measurements and cannot tell the ages of water absorbed by plants. Tritium (^{3}H), as an age-constraining tracer, has been widely used to determine the ages and recharge rates of soil water (Allision et al., 1994; Li, Si, & Li, 2018). As such, the combination of stable and radioactive water isotopes is promising in SWB partitioning and plant water identification.

The Loess Plateau of China, located in an arid and semiarid region, covered by the thickest loess in the world, has fragile ecosystems and severe erosions (Li et al., 2020; Zhu et al., 2018). Since the 1990s, the Grain for Green Project has substantially converted farmland to forestland to control soil loss (Huang & Gallichand, 2006; Wang, Yan, et al., 2021; Wang et al., 2016). In particular, apple trees have been widely planted to facilitate ecological and economic benefits (Baldi et al., 2013; Gao et al., 2021). The planting areas of apple trees had reached approximately 1.3×10^{4} km^{2} by 2016, accounting for 25% of global coverage (Wang et al., 2020). However, the planted orchards have caused negative effects on water resources (Li, Si, Wu, & McDonnell, 2018; Li et al., 2019, 2021; Shi, Huang, Ji, et al., 2021; Wang, Yan, et al., 2021; Zhang, Li, et al., 2018), such as severe soil water deficit. It is essential to systematically evaluate how afforestation influence hydrological processes.

This study is in an attempt to partition the SWB under different land use types (farmland and apple trees with varying ages), and determine the source water of root uptake of apple trees. The novelties of this study may include two aspects: (a) the stable and radioactive isotopes of water are combined to partition SWB and quantify the impacts of land use changes on soil hydrological processes, and (b) the water use strategies of apple trees under investigation can help reveal the mechanism behind the SWB changes. Specifically, each component of SWB will be quantified by combing stable and radioactive water isotopes, and then the MixSIAR model will be used to determine the water sources of apple trees over seasons and years. These results are important for understanding the hydrological processes and water uptake strategies of plants in regions with thick unsaturated zones and arid climate. Our findings will be helpful for sustainable management of water resources and vegetation restoration in the study region, and the employed methods can provide technical support for SWB partitioning in other similar studies.

2. Materials and Methods

2.1. Study Area

The study area is located at Changwu County, Shannxi Province of China (Figure 1). The study site in the tableland has a loess depth beyond 200 m (Zhu et al., 2018), and the tableland has flat surface with little runoff. The groundwater level is 84 m below surface. From the bedrock to the top, the loess deposits include three layers (Wucheng Loess with a thickness of 30–50 m covering the bedrock, Lishi Loess with a thickness of 100–150 m, and Malan Loess with a thickness of 20–30 m distributed as the topsoil). The investigated area belongs to warm temperature zone, with long-term mean annual precipitation of 585.0 mm, temperature of 9.4°C, and potential evapotranspiration of 1015.3 mm (1957–2017). Precipitation has an uneven distribution throughout the year, 68% of which falls between July and September. The main land use types include wheat, maize and apple orchards. The apple orchards cover 160.6 km^{2} in 2018, accounting for 70% of the arable land. According to a survey with local farmers, apple trees bear fruit at 4–5 years with high yields at 13–18 years, and will be cut down in 30 years or so. As typical rain-fed agriculture, all arable lands have no irrigation.

2.2. Sampling and Analyzing

The paired-plot sampling method was employed to evaluate the effects of conversion from shallow-to deep-rooted plants on SWB. Three sites were selected, including a farmland (F) and two apple orchards with different tree ages (i.e., 18 and 26 years-old trees, abbreviated as A18 and A26 hereafter), with inter-site distances <1.0 km. The sites were close enough to share similar climate, soil and hydrogeological conditions, and the differences in contents and isotopes of soil water are thus caused by vegetation change to the greatest extent. As our previous study with five replicates for each site under the same land uses demonstrated that water contents in soil profiles were similar (Huang et al., 2018), it is reasonable to collect soil samples without replication for each land use.

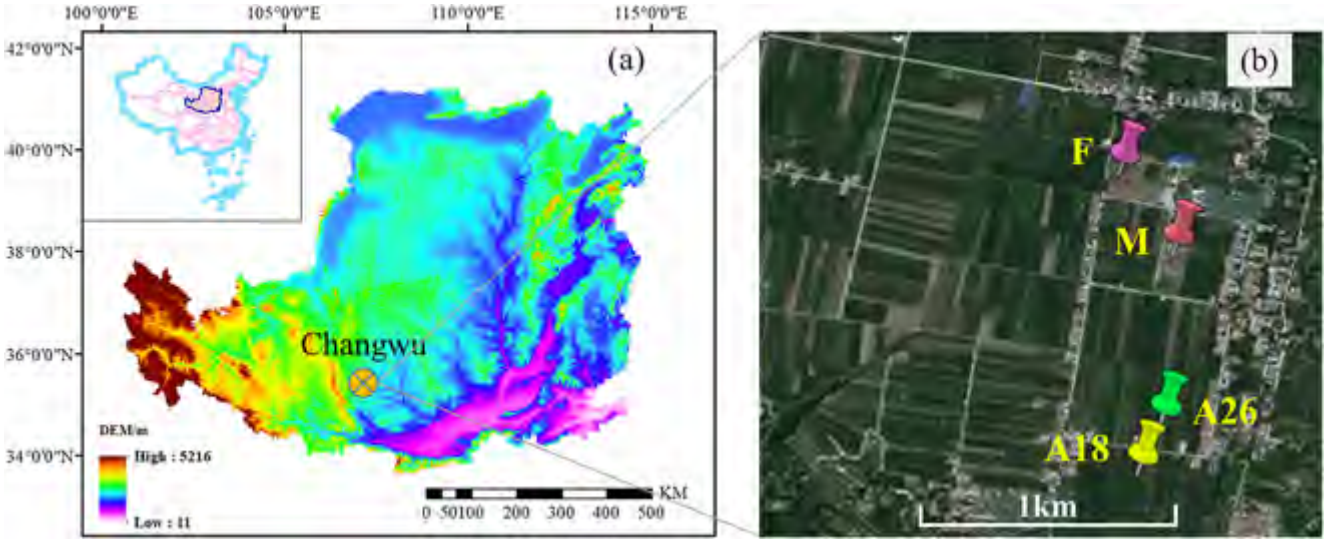

Figure 1. Location of the study area (a), meteorological station (M) and soil sampling sites (b). F, A18, and A26 respectively represents farmland, 18-and 26-year apple orchards.

We drilled a borehole up to 20 m to collect soil samples at an interval of 20 cm at each site in June 2020. Subsequently, the soil samples were collected monthly for July to October in 2020 and May to October in 2021, but only for the profile of 0–6 m. The months were selected to cover the major growing period, and the sampling depth of 6 m was selected because contents and isotopes of soil water are stabilized below that depth (Xiang et al., 2020). In particular, the local meteoric water line in our study area ($\delta^2H = 7.6\ \delta^{18}O + 9.1$) was similar with $\delta^2H = (7.67 \pm 0.11)\ \delta^{18}O + (8.76 \pm 1.00)$ in Xiang et al. (2020). The water isotopes in soils below 6 m for dynamic samplings were thus replaced by those of the first sampling.

For each soil sample, one part was stored in an aluminum box to determine gravimetric water content by oven drying method, and the second part was stored in small bottles tailored for water extraction and sealed with parafilm refrigerating at 4°C, and the remainder was stored in a plastic bottle for water extraction and tritium isotope analysis. We selected soil samples at 20-cm interval in 0–3 m soil layer, 40-cm interval in 3–6 m, and 60-cm interval below 6 m to measure $\delta^{18}O$ and δ^2H contents. The xylem samples (five replicates for each orchard) were collected from trees surrounding soil sampling site. Specifically, 1-year-old branch in each apple tree was obtained at midday, and then the xylem without phloem was cut into 3–5 cm pieces to store in 8 ml glass bottles sealed with parafilm at −20°C for stable water isotope analysis.

The liquid water in soils and plant xylems were extracted by using the automatic cryogenic vacuum distillation system (LI-2100, LICA, Beijing, China). Specifically, samples (i.e., soil, xylem) were heated at 130°C for 2 hr to evaporate completely, and then the evaporative vapor was trapped by a cryogenic system with an extraction efficiency of >98%. Precipitation samples were collected daily for isotopes measurement. The stable isotopes ($\delta^{18}O$ and δ^2H) in precipitation, soil and xylem water were determined by using the isotopic liquid water analyzer (GLA431-TLWIA, ABB Inc., Canada) with a precision of 0.3‰ for δ^2H and 0.1‰ for $\delta^{18}O$. The extracted water is 1.0–1.5 ml from each sample bottle (8 ml, ~10 g soil). About 8-ml extracted water was mixed with scintillation solution at a ratio of 8:12 for preparation, and then was stored in dark for 12hr before testing. Tritium concentration was measured by a liquid scintillation counter (Quantulus 1220, Perkin Elmer) with a detection limit of 2.0 tritium units (TU) (Shi, Huang, Yang, & Li, 2021).

The extracted plant water generally contain organic materials that may cause spectral interference when using the isotope ration infrared spectroscopy, and further result in errors in the measured isotope ratio (Millar et al., 2021; West et al., 2011; Zhao et al., 2011). The methanol and ethanol are considered as main contamination in the extracted plant analytes (Brand et al., 2009; Martín-Gómez et al., 2015; West et al., 2011), and researches indicated that the deionized water spiked with methanol and ethanol can generate correction curves for $\delta^{18}O$ and δ^2H (Schultz et al., 2011). Therefore, we developed standard curves between water isotopes and different concentrations of methanol and ethanol to correct the measured isotope ratios of contaminated samples. Specifically,

the deionized water was mixed with varying concentrations of methanol (0.001%–0.1%, $n = 25$) and ethanol (0.01%–1%, $n = 17$) (Millar et al., 2021; Schultz et al., 2011), and then the isotopes of contaminated water (three replicates for each sample) were measured by the GLA431-TLWIA isotopic liquid water analyzer. Subsequently, the isotopic biases were used to build relationships with methanol and ethanol contamination coefficients derived by the GLA431-TLWIA Post-Analysis Software. Based on these relationships, all measured isotopic values in xylem water were corrected using the correction curves.

2.3. Partitioning of Soil Water Balance

Previous studies indicated that afforestation largely decreased soil water contents and deep drainage, and further affected soil hydrological components (Ge et al., 2020; Jia et al., 2017; Zhang, Li, et al., 2018). To investigate the long-term impacts of tree planting on SWB, we partitioned each component of the following SWB equation (Equation 1) (Kool et al., 2014). For this purpose, we calculated the mean annual ΔS since the beginning of tree planting, further estimated the long-term average annual values of E and D based on the following equations.

$$P = E + T + \Delta S + D + R \tag{1}$$

where P is precipitation, mm yr^{-1}; E is evaporation, mm yr^{-1}; T is transpiration, mm yr^{-1}; ΔS is the change of soil water storage, mm yr^{-1}; D is deep drainage, mm yr^{-1}; R is surface runoff, which is ignored in this study because the sampling sites are flat with negligible runoff, mm yr^{-1}.

2.3.1. Change in Soil Water Storage and Deep Drainage

According to the measured gravimetric water contents in each soil layer, water storage can be calculated by multiplying bulk density corresponding to the soil layers. ΔS because of tree planting was estimated as the difference of S between farmland and apple orchard. Deep drainage under apple orchards (D_a) was estimated by combing ΔS with deep drainage under farmland (D_f) (Zhang, Li, et al., 2018). Specifically, the tritium peak in soil profiles represents the depth that 1963-precipitation tritium moved in the unsaturated zone (Li, Si, & Li, 2018; Tao, Li, et al., 2021), D_f can be thus estimated by Equation 2 (Phillips, 1994; Si & de Jong, 2007). Subsequently, D_a can be estimated by Equation 3 through taking out ΔS. θ stands average volumetric water content, $cm^3\ cm^{-3}$. Z_t and Z_a represent the depths of tritium peak and active rooting zone (m), respectively. According to our observed water contents and fine root length density in soil profile (Li, Si, & Li, 2018; Li et al., 2019), the value of Z_a can be represented by 2 m t is the period length since 1963, year.

$$D_f = \theta \frac{Z_t - Z_a}{t} \tag{2}$$

$$D_a = D_f - \Delta S \tag{3}$$

2.3.2. Soil Evaporation Loss

Considering the inputs (I) and outputs of water are in long-term equilibrium, Equation 1 can be expressed as Equation 4 with the assumption that all precipitation infiltrating into soil without surface runoff. Subsequently, a steady-state isotope mass balance model can be expressed as Equation 5, which is similar to other methods in partitioning ET (Al-Oqaili et al., 2020; Gibson & Edwards, 2002; Good et al., 2014). δ_I, δ_E, δ_T, δ_s, are respectively the isotopes of input water, evaporated water, transpiration, and soil water, ‰.

$$I = E + T + D + \Delta S \tag{4}$$

$$I\delta_I = E\delta_E + T\delta_T + (D + \Delta S)\delta_S \tag{5}$$

The steady-state isotope mass balance model was assumed to be balanced by fractionated (E) and non-fractionated (T and D) losses. Therefore, we used soil water isotopes above the depth reflecting the maximum evaporation effect of tree planting to calculate evaporation loss. Theoretically, the xylem water isotope can well represent isotope signal in transpiration. However, recent studies indicated that plant xylem water isotopes have an isotopic fractionation during cryogenic water extraction or root water uptake (Barbeta et al., 2020; Chen et al., 2020). Further, the xylem water isotopes are mixtures of soil water isotopes of different soil layers including below the abovementioned maximum evaporation depth. As such, the xylem water isotopes would not match with the

transpiration isotope signal from the surface to maximum evaporation depth. Therefore, we used the δ_s above the maximum evaporation depth to substitute δ_T. As such, the fraction of evaporation loss to the input can be estimated with Equation 6 (Al-Oqaili et al., 2020; Xiang et al., 2021). For evaporation estimation, it is very important to determine a critical depth reflecting the maximum evaporation effect of tree planting. We conducted this step by comparing the time period represented by soil water tritium peak and the ages of apple trees. The profile from the surface to soil water tritium peak depth represents soil water movement since 1963, but the apple trees were planted in recent 30 years. As such, the depth of 6 m contains water of ~50 years old, the infiltration rates can be estimated by an equation similar as Equation 2 (i.e., infiltration rates = $(Z_t - Z_a)/t$ = (6−2 m)/50 years = 8.0 cm year^{-1}). The depth covering the period of land use change can thus be estimated as Z_a + 8.0 cm year^{-1} × 30 years/100 = 4.4 m. Therefore, it is reasonable to use the depth profile above tritium peak depth (i.e., 0–6 m) to reflect the maximum evaporation depth. Consequently, the stable oxygen isotope within 0–6 m were used to estimate *E*/*I*, which refers as the long-term average annual evaporation rates. δ_I can be calculated with soil water evaporation line and Local Meteoric Water Line by a Bayesian-type statistical approach (Bowen et al., 2018). It should be noted that the soil water evaporation line was not directly regressed from soil water isotopes, but based on the Craig-Gordon model (Benettin et al., 2018; Bowen et al., 2018). δ_s was derived from the measured isotopic compositions in the sampled soils above 6 m. δ_E was estimated by the Craig-Gordon model (Craig & Gordon, 1965).

$$\frac{E}{I} = \frac{\delta_I - \delta_S}{\delta_E - \delta_S} \tag{6}$$

where h and δ_A respectively represent relative humidity and isotopic composition of the atmospheric vapor, $\delta_A = (\delta_P - \varepsilon^+)/\alpha^+$, ‰ (Gibson & Reid, 2014). δ_P is the monthly volume-weighted isotopic values of precipitation, ‰; ε^+ and α^+ are the temperature-dependent equilibrium fractionation factors, ‰, $\varepsilon^+ = (\alpha^+ - 1) \times 1000$. ε_k is kinetic fractionation factor calculated by the methods in Benettin et al. (2018). The monthly mean temperature and relative humidity for 1957–2017 were used to estimate the ε^+ and ε_k.

$$\delta_E = \frac{(\delta_s - \varepsilon^+)/\alpha^+ - h\delta_A - \varepsilon_k}{1 - h + \varepsilon_k/1000} \tag{7}$$

2.3.3. Vegetation Transpiration

Based on Equation 1, T can be indirectly calculated as the residual of known components.

2.4. Determining Source Water for Root Uptake

To reveal the mechanism of SWB changes, we explored the dynamics of root water uptake of apple trees. In this study, as the groundwater is too deep to be absorbed by plants, soil water is considered as the only subsurface source water. The contributions of water stored in different soil layers to xylem water of apple tree were determined using a Bayesian model framework MixSIAR (Stock & Semmens, 2016; Stock et al., 2018). To avoid the errors in plant water source identification from isotope fractionation during water extraction or root water uptake (Barbeta et al., 2020; Chen et al., 2020; Vargas et al., 2017), a correction method (Equation 8), proposed by Barbeta et al. (2019), was employed.

$$\text{SW} - \text{excess} = \delta^2\text{H} - a_s\delta^{18}\text{O} - b_s \tag{8}$$

where a_s and b_s are the slope and intercept of the fitted line for all soil water isotope data for a given site and date, respectively. The δ^{18}O and δ^2H represent the isotope of xylem water collected on that site at that date. The SW-excess is an indicator of δ^2H offsets between xylem water and the corresponding soil water lines. Positive SW-excess indicates xylem water are more enriched than soil water line, while negative values indicate more depleted xylem water relative to soil water line. The directly measured isotopes in xylem water were defined as the measured values, while the correction was presented the corrected isotopes. The measured and corrected δ^2H of xylem water of apple tree during two growing seasons were shown in Table 1.

Based on vertical distributions and temporal dynamics of water content and water isotopes (δ^{18}O, δ^2H) in soil profiles, the entire soil profiles were divided into five potential water sources (0–0.8 m, 0.8–2 m, 2–4 m, 4–6 m, and >6 m). Specifically, the water contents and isotopes in 0–0.8 m vary frequently because of the combined

Table 1
The Measured and Corrected δ^2H of Xylem Water of Apple Tree Over the Growing Seasons

Apple orchards	A18		A26	
Sampling date	Measured δ^2H	Corrected δ^2H	Measured δ^2H	Corrected δ^2H
2020-6-24	−57.3 ± 3.6	−55.3 ± 4.1	−59.7 ± 2.1	−52.8 + 2.1
2020-7-30	−62.3 ± 3.7	−58.7 ± 3.3	−60.6 ± 1.8	−55.0 ± 2.0
2020-8-30	−88.1 ± 11.3	−80.9 ± 9.8	−92.4 ± 6.2	−85.7 ± 5.6
2020-9-28	−80.5 ± 7.4	−77.5 ± 6.6	−86.6 ± 2.2	−81.7 ± 2.5
2020-10-30	−79.0 ± 12.4	−69.6 ± 12.4	−76.6 ± 6.0	−70.0 ± 6.0
2021-5-21	−71.2 ± 1.1	−66.7 ± 1.0	−66.7 ± 0.6	−62.5 ± 0.6
2021-6-30	−69.9 ± 2.9	−66.7 ± 2.9	−64.8 ± 4.0	−57.8 ± 4.2
2021-7-27	−66.4 ± 0.2	−64.2 ± 0.1	−64.9 ± 1.8	−59.7 ± 1.8
2021-8-27	−73.9 ± 0.3	−72.9 ± 0.9	−67.4 ± 0.2	−64.9 ± 0.7
2021-9-21	−81.9 ± 0.2	−75.7 ± 0.2	−75.5 ± 0.4	−69.9 ± 0.9
2021-10-27	−87.8 ± 0.9	−80.0 ± 1.2	−87.0 ± 0.4	−82.4 ± 0.6

effects of wet events and evaporation, while they have little changes in 2–4 m, and are only affected by extreme precipitation events in 4–6 m. According to tritium peak depth, the water in layers >6 m is likely to originate from precipitation of five decades ago. Therefore, based on the $\delta^{18}O$ and corrected δ^2H, we estimated the contributions of potential water source to xylem water to determine water uptake strategy of apple tree. The average isotopes with standard deviations in each potential water source and xylem water were respectively used as single and mixed sources in the model.

2.5. Uncertainty and Statistical Analysis

Precipitation amounts, soil water contents and isotopes, as well as xylem water isotopes, exist temporally variability, and thus introduce uncertainties to SWB partitioning. Therefore, the error propagation analysis was used to quantify the related uncertainties (Equations 9 and 10), of which a_i the uncertainty of the related variable (standard deviation), is the parameter of the error propagation.

$$\sigma_y = \left(\frac{\partial f}{\partial x_1}\right)^2 \sigma {x_1}^2 + \left(\frac{\partial f}{\partial x_2}\right)^2 \sigma {x_2}^2 + \cdots + \left(\frac{\partial f}{\partial x_n}\right)^2 \sigma {x_n}^2 \quad (9)$$

$$\text{If } \frac{\partial f}{\partial x_i} = a_i \, (i = 1, 2\ldots, n), \text{ then}$$

$$\sigma_y = {a_1}^2 \sigma {x_1}^2 + {a_2}^2 \sigma {x_1}^2 + \cdots + {a_n}^2 \sigma {x_n}^2 \quad (10)$$

The significance of the differences in variables for both orchards and years was tested using the *t*-test. The differences in the isotopes of xylem water and soil water, and contribution proportion of different soil layers to xylem water under different land use types were tested by the one-way analysis of variance (ANOVA). The statistically significant difference was indicated by $p < 0.05$.

3. Results

3.1. Contents and Isotopes of Soil Water

The soil profiles collected at the first time (i.e., June 2020) up to 20 m deep were used to show the overall vertical variability in water contents and isotopes. The soil water contents above 2 m were more variable than those of 2–4 m, but they were overall similar for different land use types (Figure 2a). However, the water contents and storages below 6 m showed big differences under three land uses. Specifically, the water stored in the whole profile was the lowest under A26 (4,130 mm), intermediate under A18 (4,571 mm) and the largest under F (4,817 mm). It suggests that apple trees had negative impacts on soil water storage, and will probably result in further changes in soil hydrological processes. Figures 3a and 3b showed the temporal variations of soil water contents under apple orchards during two growing seasons in 2020–2021. The water contents in 0–2 m soil layers varied largely with growing season, because of the interaction of precipitation, evaporation and root water uptake. Specifically, the shallow soil water increased in the rainy season (August–October), but decreased in the dry season (May–July). However, the variations of soil water contents in 2–4 m were relatively small than those above 2 m, since they are may be mainly affected by heavy wet events (Ji et al., 2021). In Particular, the soil water contents above 5 m increased significantly in 27 October 2021 because of the large precipitation amounts of 230 mm in October.

The $\delta^{18}O$ and δ^2H of soil water above 4 m showed a large fluctuation, but were stabilized below 4 m (Figures 2b and 2c) for the first samplings. Further, the monthly soil profiles indicated that soil water isotopes had similar temporal variations under A18 and A26 during two growing seasons. The water isotopes in shallow soils above 2 m was more depleted in rainy season, but more enriched in dry season. Specifically, the $\delta^{18}O$ and δ^2H in 0–0.8 m changed dramatically (−6.1‰ to −18.2‰ for $\delta^{18}O$, and −47.8‰ to −128.7‰ for δ^2H), most likely being depleted by wet events or enriched by evaporation. But they were was less variable in 0.8–2 m (−7.3‰ to −14.9‰ for $\delta^{18}O$, and −50.5‰ to −108.5‰ for δ^2H) than those above 0.8 m. The $\delta^{18}O$ and δ^2H varied slightly

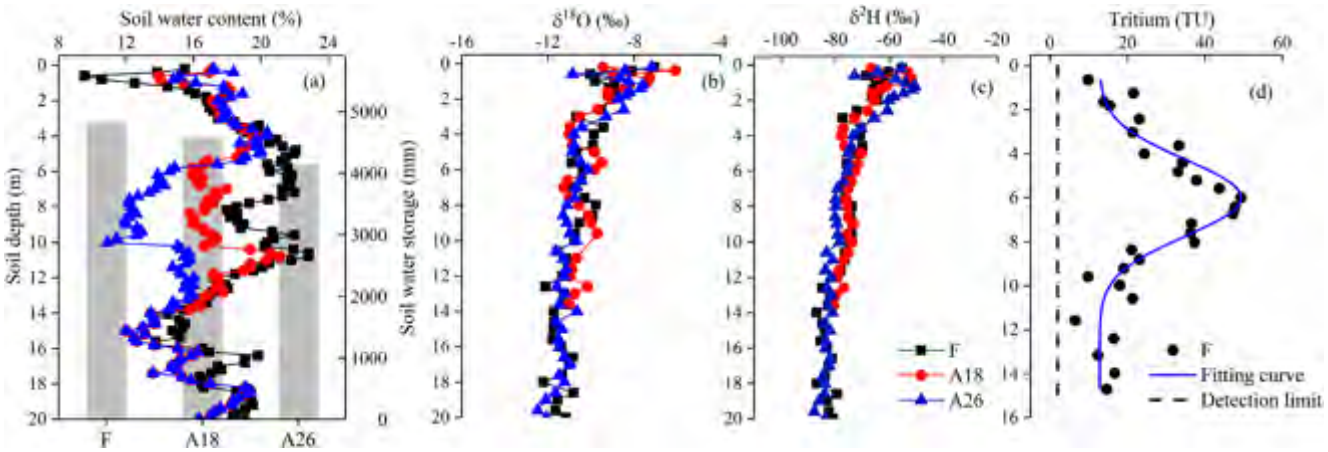

Figure 2. The contents of (a) water, (b) $\delta^{18}O$, (c) $\delta^{2}H$, and (d) tritium in soil profiles. Figure (a–c) shares the same legend presented in (c). F, A18, A26 respectively represent farmland, 18-year apple orchard, and 26-year apple orchard. The gray bar in (a) indicates soil water storage. Tritium data under farmland in (d) derived from Li, Si, & Li, 2018.

in 2–4 m soil layers (−7.7‰ to −11.8‰ for $\delta^{18}O$, −57.0‰ to −83.0‰ for $\delta^{2}H$) but relatively stabilized below 4 m (−9.5‰ to −11.8‰ for $\delta^{18}O$, and −61.2‰ to −86.1‰ for $\delta^{2}H$) (Figures 3c and 3d). This further confirmed the assumption that deep soil water isotopes below 6 m can hardly be affected by short-term infiltration or evaporation, and demonstrated the partitioning of soil profiles was reasonable to calculate the contributions of potential water source to xylem water. The ^{3}H in soil water under farmland exhibited a clear peak at the depth of 6 m (Figure 2d), suggesting that water moves downward by piston flow in the unsaturated zone (Li, Si, & Li, 2018; Phillips, 1994). As the tritium peak value corresponds to the tritium input of the 1963-precipitation, the soil profiles can be partitioned into two parts. Specifically, the depth profile below 6 m had soil water originating from precipitation older than ∼50 years, while the profile of 0–6 m had soil water younger than ∼50 years.

3.2. Isotope of Precipitation and Xylem Water

The total precipitation in 2019, 2020, and 2021 was 659.6, 598.0, and 870.2 mm, respectively. Compared with the long-term average (585.0 mm, 1957–2017), 2019 and 2021 were wet years, while 2020 was a normal year. The monthly volume-weighted precipitation isotopes had large seasonal variations with $\delta^{18}O$ ranging from −3.6‰ to −18.4‰ and $\delta^{2}H$ ranging from −122.7‰ to −20.6‰ (Figure 4). Overall, the precipitation isotopes were

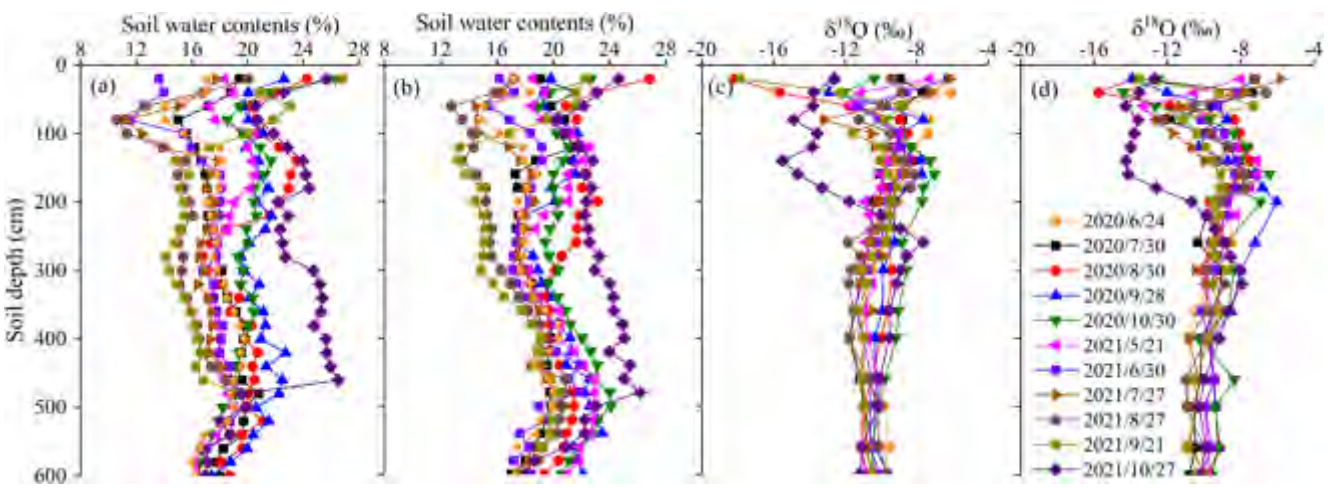

Figure 3. The variations of soil water content under (a) A18 and (b) A26, and water isotopes under (c) A18 and (d) A26 during two growing seasons in 2020–2021. Figure (a–d) shares the same legend presented in (d).

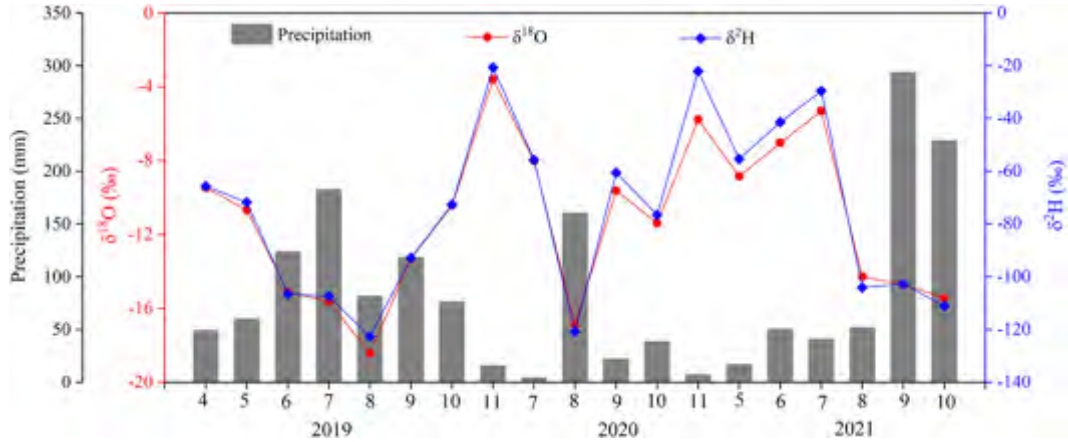

Figure 4. The amount and monthly-weighted isotopic values of precipitation during 2019–2021.

depleted in rainy seasons but enriched in dry seasons, and the seasonal variations indicated the amount effect of precipitation isotopes.

For the xylem water isotopes in growing seasons of 2020 and 2021, the measured $\delta^{18}O$ of A18 ranged from −6.0‰ to −12.2‰ with a mean value of −9.1‰ ± 0.8‰, while the measured and corrected $\delta^{2}H$ ranged from −57.3‰ to −88.1‰ with a mean value of −74.4‰ ± 9.6‰ (Table 1), and −55.3‰ to −80.0‰ with a mean value of −72.1‰ ± 8.9‰, respectively. The measured $\delta^{18}O$ of A26 ranged from −7.3‰ to −12.7‰ with a mean value of −9.1‰ ± 0.5‰, while the measured and corrected $\delta^{2}H$ ranged from −59.7‰ to −92.4‰ with a mean value of −72.9‰ ± 10.9‰ (Table 1), and −52.8‰ to −82.4‰ with a mean value of −70.3‰ ± 11.7‰, respectively (Figure 5). Compared to the measured values, the corrected values were more enriched with a mean offset value of −5.0‰ ± 1.9‰. The xylem water isotopes had significant differences in seasons ($p < 0.05$), but the differences between trees with different ages were not significant ($p > 0.05$). The xylem water isotopes were more abundant in dry seasons than those in rainy seasons, implying that apple trees may have various water sources over the growing season.

3.3. Partitioned Soil Water Balance Components

Because of the interannual and monthly differences in precipitation, the soil water contents above 2 m had large variations under three land uses (Figure S1 in Supporting Information S1), and the water storage was thus different between farmland and orchards over the growing season. Based on the dynamic observations of soil water

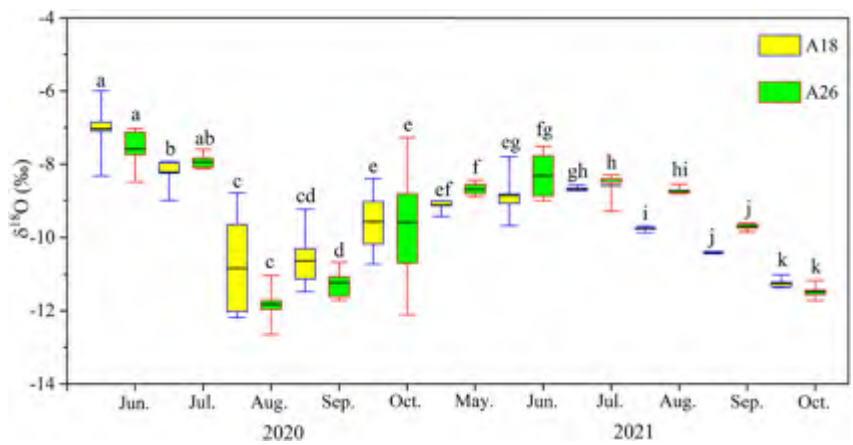

Figure 5. The values of $\delta^{18}O$ of plant xylem during growing period. In each boxplot, the lower boundary of the box shows the 25th percentile and the upper boundary shows the 75th percentile, and the lines across the boxes indicate the mean values. Different letters next to the box plot indicate significant differences in $\delta^{18}O$ values of xylem water ($p < 0.05$).

Table 2
The Estimated Hydrological Variables Under Different Land Uses

Land use types	P (mm yr^{-1})	ΔS mm yr^{-1}	D mm yr^{-1}	ET mm r^{-1}	E mm yr^{-1}	T mm yr^{-1}	E/ET %	T/ET %	ET/P %
F	585 ± 128	–	27.9 ± 0.4	557.1 ± 128	179.6 ± 91.5	377.5 ± 157.3	32 ± 18	68 ± 32	95 ± 30
A18	585 ± 128	−13.6	14.3 ± 0.8	584.4 ± 128	148.6 ± 115.7	435.8 ± 172.5	25 ± 21	75 ± 34	100 ± 31
A26	585 ± 128	−26.4	1.5 ± 0.9	609.9 ± 128	125.8 ± 103.1	484.1 ± 164.4	21 ± 17	79 ± 32	104 ± 32

Note. P: annual average precipitation; ΔS: soil water storage deficit; D: deep drainage; ET: evapotranspiration; E: evaporation; T: transpiration.

contents within 0–6 m over both growing seasons, the estimated ΔS was respectively 133.9, 223.6, and 192.0 mm in 2020, and 9.0, 12.5 and −70 mm for F, A18 and A26 in 2021 (Table S1 in Supporting Information S1). Compared to farmland, the ΔS was 46.6 and −10.9 mm for A18 and A26 in two growing seasons, respectively. The short-term changes of SWB in shallow layers are controlled by precipitation.

However, for the long-term changes in SWB, the deep soil layers should be incorporated to fully reflect the root water uptake. In consequence, the long-term effects of land use change on each component were estimated using Equation 1–7. With the reference farmland, ΔS was −13.6, and −26.4 mm yr^{-1} under A18 and A26, respectively. The estimated D under F, A18, and A26 was 27.9 ± 0.4, 14.3 ± 0.8, and 1.5 ± 0.9 mm yr^{-1}, respectively (Table 2). Compared with farmland, D and S under two orchards decreased significantly, suggesting that tree planting can prevent deep drainage by absorbing soil water. Based on the SWB equation (Equation 1), the estimated mean annual ET under F, A18, and A26 was respectively 557.1 ± 128, 584.4 ± 128, and 609.9 ± 128 mm, accounting for 95%–104% of mean annual precipitation (Table 2), which suggests tree planting can produce imbalance in soil hydrological processes. Furthermore, the estimated mean annual E under F, A18, and A26 was respectively 179.6 ± 91.5, 148.6 ± 115.7, and 125.8 ± 103.1 mm accounting for 32 ± 18%, 25 ± 18%, and 21 ± 17% of total ET, while the annual average T under F, A18 and A26 was respectively 377.5 ± 157.3, 435.8 ± 172.5 and 484.1 ± 164.4 mm, accounting for 68%–79% of total ET. The mean annual T/ET under F, A18, and A26 was respectively 68 ± 32%, 75 ± 34% and 79 ± 32%, which increased with increasing ages of apple trees. It appeared that most SWB components decreased to satisfy the increased T from root water uptake.

3.4. Identified Source Water of Apple Trees

The water source of plants can be qualitatively determined through the comparison in the isotopes of soil water and xylem water, and their intersection points can be regarded as the potential water source. The potential water source showed significant differences for the sampling date and apple tree age (Figures 6 and 7), suggesting apple trees were likely to obtain water from different soil layers and varied with the growing season. Specifically, apple trees mainly used shallow soil water within 0–2 m at the beginning of the growing season (May–July), while they absorbed water from the whole soil profiles but dominated by deep soil water below 2 m in late growing season (August–October). The δ^2H and $\delta^{18}O$ in soil water showed a similar variation trend down the vertical profiles, and the intersection for both values was consistent with those of xylem water. As such, the δ^2H and $\delta^{18}O$ values can be used to calculate the contribution fractions of the potential water source to xylem water.

To further explore how root water uptake affects SWB components, we quantified the contributions of potential water sources to xylem water (Figure 8). Overall, the apple trees with different ages had similar water use patterns during the study period. They mainly absorbed water in soil layer of 0–2 m at the beginning of growing season (May–July), and the contributions were 71% and 65% for A18 and A26, respectively ($p < 0.05$). However, in late growing season (August to October), the soil water below 2 m contributed 65% and 59% to xylem water of A18 and A26, respectively ($p < 0.05$); particularly, the soil water below 6 m had contributions of 24% and 22% for A18 and A26, which represented the water older than 50 years. It appeared that apple trees shifted water source from shallow soil above 2 m to deep soil below 2 m within the growing season.

The water use strategies were slightly different between 2 years. In the growing season of 2020 (normal year), the contributions of soil water below 2 m were 42%, and 43% for A18 and A26, respectively ($p > 0.05$). Although similar patterns of water uptake were observed in 2021 (wet year), the fraction of deep soil water below 2 m under A18 and A26 in 2021 was respectively 23% and 18% higher than that in 2020, especially in the beginning of growing season ($p < 0.05$). It indicated that the water use strategies of apple trees may be affected by both

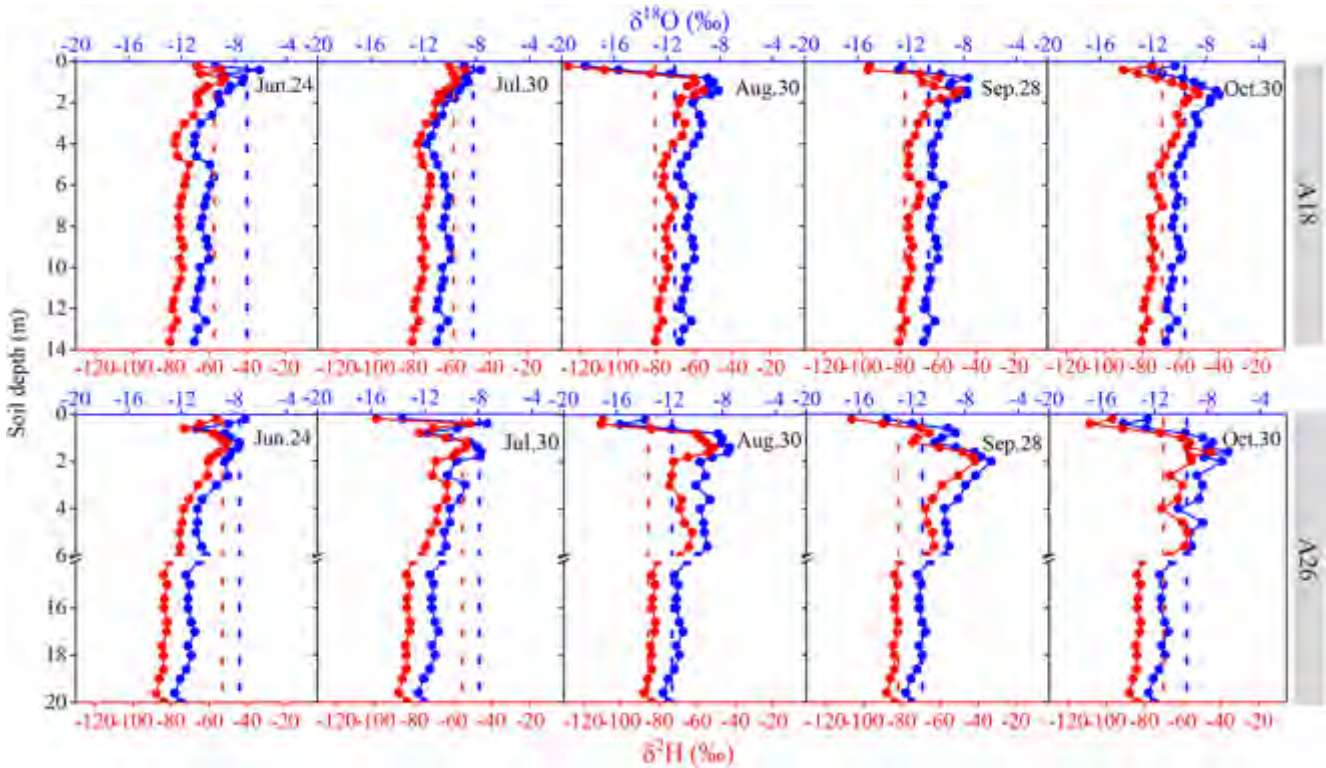

Figure 6. Seasonal variations of δ^2H and $\delta^{18}O$ in soil water under A18 and A26, and the relationships with xylem water isotopes in 2020. Solid lines represent soil water isotopes and the dashed lines represent xylem water isotopes.

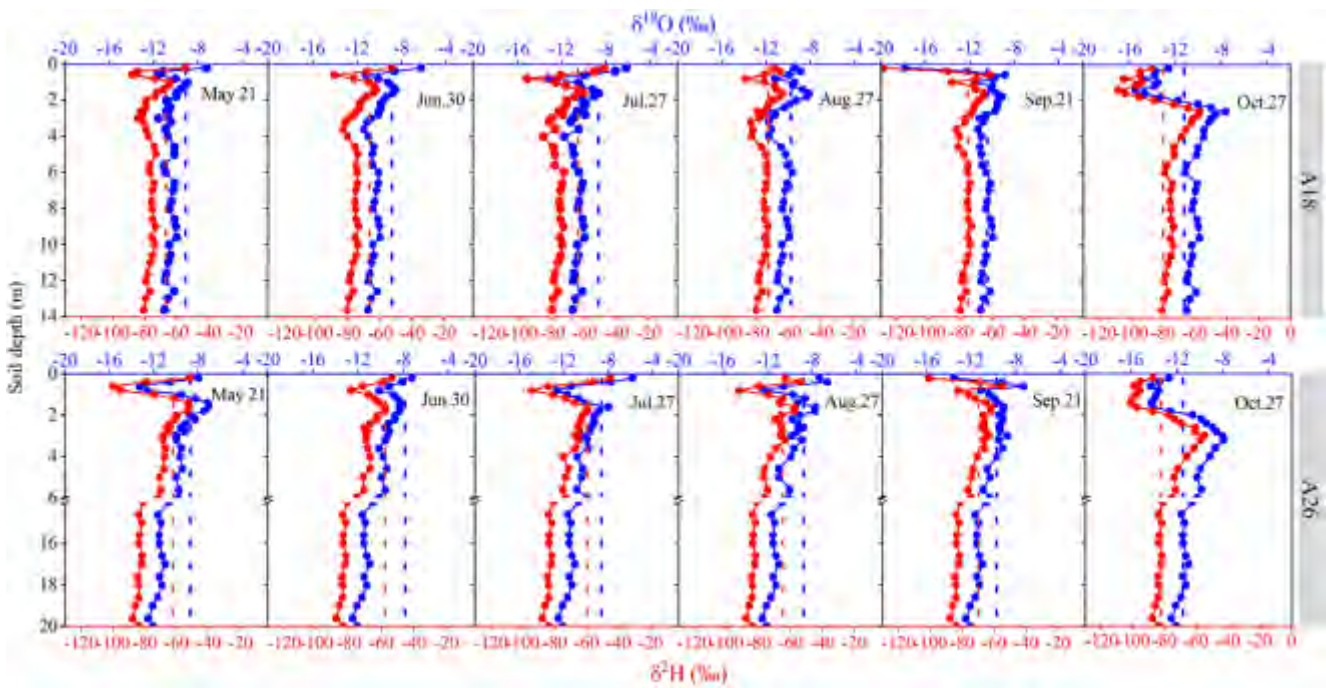

Figure 7. Seasonal variations of δ^2H and $\delta^{18}O$ in soil water under A18 and A26, and the relationships with xylem water isotopes in 2021. Solid lines represent soil water isotopes and the dashed lines represent xylem water isotopes.

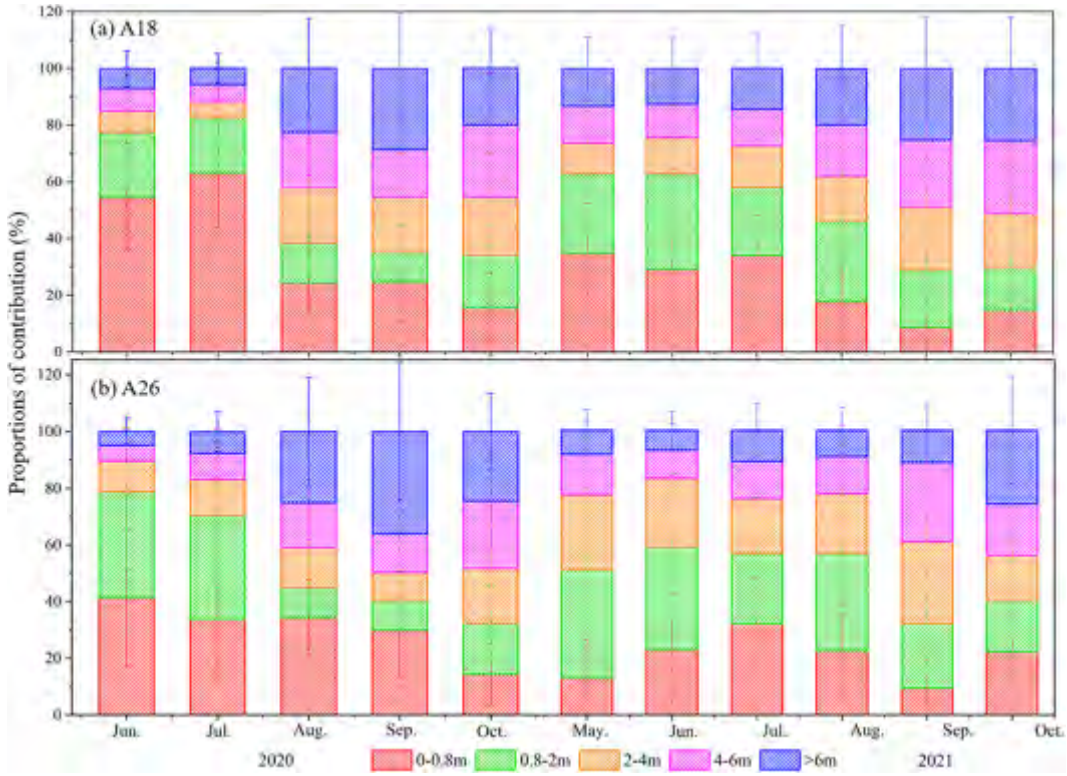

Figure 8. Seasonal variations in the proportional contributions of water from different soil layers to xylem water of (a)18- and (b) 26-years old apple trees on the basis on calculation of oxygen and hydrogen stable isotopes. The error bar represents the standard deviation of contribution proportion of soil water to root water uptake in each soil layer.

physiology and climate. This can be confirmed by previous studies indicating that the water use strategies of plant species have strong sensitivity to photosynthesis, stomatal conductance, and vapor pressure deficit (Flo et al., 2021; Lanning et al., 2020). In particular, the water use strategies were related to the ages of apple trees. Specifically, the absorbed water from soil layers below 2 m by A26 (35%) was significantly higher than that by A18 (30%) at the beginning of the growing season in 2020–2021 ($p < 0.05$). Particularly, the contribution of soil water below 2 m for A26 was 18% higher than that for A18 in 2021 (45% for A26 vs. 38% for A18).

4. Discussion

4.1. Uncertainties in Partitioning of Soil Water Balance and Plant Water Sources

Water availability in soils is crucial for the survival and growth of plants, and it is important to understand how plant interact with water in different bodies (Ding et al., 2021; Gessler et al., 2021). Partitioning of SWB is an effective way for this purpose but remains challenging (Jasechko et al., 2013; Shao et al., 2021). In this study, we employed stable and radioactive water isotopes to decompose each component of SWB. First, with farmland as reference, ΔS under apple trees was directly calculated by the field measured data, which is an important component in SWB under vegetation changes but neglected in most previous studies (Koppa et al., 2021; Ning et al., 2019; Shao et al., 2021; Zhang, Yang, et al., 2018). Subsequently, we estimated D under apple trees by combining ΔS with deep drainage under farmland (Equation 3). This method has been demonstrated to be robust for estimating recharge rates under deep-rooted plants (Huang et al., 2019; Li, Si, & Li, 2018; Zhang, Li, et al., 2018). Based on the estimated ΔS and D, ET can be inversely calculated by SWB equation (Equation 1). Further, the ratio of evaporation loss was estimated by using the steady-state isotopes mass balance model (Equation 6), thus ET can be easily partitioned into E and T. As such, the components of SWB were mostly estimated with direct observation, and the results under different types should be reliable. However, if the xylem water isotopes are directly used as inputs for T estimation, it may lead to large uncertainties. The isotopes of soil water within 0–6 m (−9.5‰ for $\delta^{18}O$ and −65.3‰ for $\delta^{2}H$) were significantly different with those in the measured

Table 3
Partitioned Soil Water Balance Based on Multiple Methods and Scales Under Different Vegetation Types

No	Location	Vegetation	Methods	*P*, mm	*D*, mm	*ET*, mm	*E*/*ET*, %	*T*/*ET*, %	Reference
1	Changwu, Shaanxi	Wheat, Apple	HYDRUS	580	0–12	566–578	–	–	Li et al. (2019)
2	Jinghe, Gansu	Grass, Forest	Sap flow & ML	548	0–47	457–619	–	–	Schwarzel et al. (2019)
3	Daning, Shanxi	Wheat, Apple	Isotope & SWB	528	0–37	502–600	31–41	59–69	Shi, Huang, Ji, et al. (2021)
4	Boreal forest	Forest	Meta-analysis	500	–	356	–	65 ± 18	Schlesingera and Jasechko (2014)
5	North America	Grass, Forest	uWUE	300–500	–	–	31–48	52–69	Zhou et al. (2016)
6	Laboratory	Grass	Isotope & HYDRUS	–	–	–	12–27	64–78	Sutanto et al. (2012)
7	Arizona, USA	Woodland	RFM & BECM	261	–	662	22–44	56–78	Scott et al. (2020)
8	southwest China	Forest	Isotopes	935	–	–	19–41	59–81	Han et al. (2022)
9	Changwu, Shaanxi	Wheat, Apple	Isotopes & SWB	585	2–28	557–610	21–32	68–79	This study

Note. *P*: precipitation; *D*: deep drainage; *ET*: evapotranspiration; *E*: evaporation; *T*: transpiration; ML: micro-lysimeter; SWB: soil water balance; uWUE: the concept of underlying water use efficiency; RFM: random forest model; BECM: the best-fitted ecosystem conductance model.

(−7.0‰ for $\delta^{18}O$ and −58.5‰ for $\delta^{2}H$) or corrected xylem water (−7.0‰ for $\delta^{18}O$ and −54.0‰ for $\delta^{2}H$) under both orchards ($p < 0.05$). Further, if *T* is calculated using Equation 5 based on the measured and corrected xylem water isotopes, and the estimated *T* was quite different from that calculated by Equation 1. Specifically, with dynamically analyzed xylem water isotopes, the dynamic *T* estimated by oxygen isotope has a range of 318.7–536.9 mm year^{-1}, and the values for measured and corrected hydrogen isotope are 148.0–280.4 mm year^{-1} and 160.0–317.6 mm year^{-1}, respectively. Therefore, direct employment of xylem water isotopes for *T* estimation is not recommended for long-term SWB analysis, but may have potential in dynamic *T* estimation unless *E* can be estimated dynamically.

To further verify the reliability of our methods, we compared the results of this study with other studies based on different methods or scales (Table 3). The estimated *D* was 1.5–27.9 mm year^{-1} under three land uses, consistent with most studies calculated by different methods in this area (Li, Si, & Li, 2018) (Table 3). The estimated *ET* was 557.1–609.9 mm year^{-1}, which overlaps with the results modeled by HYDRUS-1D in the same area (566–578 mm year^{-1}) (Li et al., 2019), and is close to the global average of 541 mm year^{-1} estimated with the Budyko framework (Wang, Cheng, et al., 2021), as well as 568 mm year^{-1} over vegetated lands estimated from MODIS products (Yu et al., 2021).

We further estimated the ratio of *E* or *T* to total *ET*, respectively. In this study, the estimated *E*/*ET* was 21%–32%, falling within the range of 20%–40% from global-scale meta analysis (Kool et al., 2014). The *T*/*ET* of 68%–79% in this study is also comparable with other studies based on various *ET* partitioning methods (Table 3). In particular, it was similar to the results of forest based on field measurement (65%–76%), and isotope-based methods or water use efficiency-based methods in the similar region (55%–69%) (Shi, Huang, Ji, et al., 2021; Zhou et al., 2018), as well as the value of 67 ± 14% for temperate deciduous forest from a compilation of previous *ET* partitioning studies (Schlesingera & Jasechko, 2014).

Therefore, combining content, stable and radioactive isotopes of soil water, this study presents an effective method for *ET* and SWB partitioning. As for the determination of plants water sources, we have considered $\delta^{2}H$ fractionation of the xylem water. The soil water presents the only source for plant water uptake in the study area, so the measured isotopes of xylem water can be corrected with the offset values of SW-excess, calculated by the slope and intercept of the fitted line for soil water isotopes for each sampling period (Equation 8) (Barbeta et al., 2019). Our results indicated significant differences between the corrected and measured values ($p < 0.05$) and the measured $\delta^{2}H$ were more depleted than the corrected values (Table 1). This is similar to the conclusion of Chen et al. (2020) who showed that the cryogenic extraction method can resulted in $\delta^{2}H$ depletion of plants xylem water. As such, our estimated source water of apple trees should be reliable based on the corrected $\delta^{2}H$ and measured $\delta^{18}O$.

4.2. Water Uptake Strategy of Apple Trees With Different Ages

Apple trees have been widely planted around the world because of high economic benefits (Baldi et al., 2013; Gao et al., 2021). However, how they extract soil water has not been fully understood, which is important for assessment of adaptability to drought and understanding ecohydrological processes. Previous studies indicated that different species with various rooting systems may have different water uptake strategies (Brinkmann et al., 2019; Jackson et al., 2000; Wang et al., 2020), as well as different impacts on soil hydrological processes. However, a few studies indicated that root water uptake was not necessarily in line with root density profiles (Volkmann et al., 2016; Werner & Dubbert, 2014). As such, we calculated the contributions of different soil layers to root water uptake of apple tree. Our results indicated that apple trees with different ages mainly absorbed shallow soil water (0–2 m) at the beginning of growing season, while they extracted more water from soils below 2 m in late growing season (Figure 8), which is consistent with Wu et al. (2022), who reported that apple trees increased their uptake of deep soil water below 4 m in August to September in similar loess regions. This suggests that apple trees shifted their water source from shallow (0–2 m) to deep soils (below 2 m) over the growing season, which is different from Gessler et al. (2021) who found that Beech reduced water uptake from the drying topsoil during drought. The water use strategies of apple trees may be related to both phonologies and precipitation. Specifically, apple trees require little water to meet the growth at the beginning of growing season (May to July) because of the small leaf area index (Tao, Neil, & Si, 2021), but they need more water to meet high water-consumption for transpiration and photosynthesis in August to October because of increasing leaf area, vapor pressure deficit and photosynthesis (Anderson-Teixeira et al., 2022; Flo et al., 2021; Lanning et al., 2020). In addition, the magnitude of water absorbed from shallow (0–2 m) or deep soil layers below 2 m may be related to precipitation. Particularly, the high contributions of shallow soil water above 2 m in May to July in this study is due to the large water contents in shallow soil recharged by heavy precipitation in 2019.

Trees have high plasticity in the vertical distribution of water uptake under seasonally dry environment (Brinkmann et al., 2019; Ding et al., 2021; Miguez-Macho & Fan, 2021; Wang et al., 2020). As a result, tree species with deeper root systems (e.g., *F. excelsior*, *F. sylvatica*, and *A. pseudoplatanus*) can extract more water from deeper soil layers during drought (Brinkmann et al., 2019). These findings are further confirmed by our study, that is, an increasing fraction of water was taken from deeper soil layers over the growing season. Moreover, our results indicated that apple trees used about 23% old water from deep soils below 6 m in both normal and wet years, and older trees used more old water (ANOVA, $p < 0.05$). In particular, our previous study used tritium to explore apple source water and found that the apple trees under investigation were absorbing water of 29 years old (Zhang et al., 2017). As such, it seems that water uptake strategy of apple trees is different from some economic species (e.g., *Picea abies*, *H. rhamnoides*, *Beech*), which reduces the fraction of water uptake by regulating stomates under drought conditions (Brinkmann et al., 2019; Gessler et al., 2021; Wang et al., 2019). Our results about water use strategy can be further confirmed by previous studies about root systems of apple trees, which found that old apple trees had the maximum roots depth of 23 m and 80% of fine root length density were distributed in deep soils below 2 m (Li, Si, Wu, & McDonnell, 2018; Tao, Neil, & Si, 2021). This further indicated that old apple trees with deep roots extracted more water from deep soils related to young trees with shallow roots.

4.3. Links Between Soil Water Balance and Water Uptake Strategy

Clarifying the relationship between plant water uptake strategies and SWB is important for sustainable afforestation and water resources management (Evaristo et al., 2015; Sprenger et al., 2016). In this study, the partitioned SWB indicated that farmland transferred into apple orchards significantly increased soil water deficit, which was consistent with previous studies related to the link of soil water with afforestation (Deng et al., 2020; Huang & Shao, 2019; Jia et al., 2017). In particular, we found that apple trees largely increased T but decreased D and E relative to farmland (Table 2). These findings indicated that the changes in SWB appeared to be closely related to root water uptake of trees.

First, apple trees shift their water sources from shallow (0–2 m) to deep soil layers (below 2 m) to obtain more water to meet transpiration demand. Even in a wet year (2021), apple trees absorbed ~40% water from deep soils below 4 m (Figure 8). Moreover, previous studies indicated that deep soil water below 6 m under orchards was hard to be recharged by normal precipitation events (Ji et al., 2021; Xiang et al., 2020). Second, apple trees with different ages have different water uptake strategies; in particular, older apple trees tend to use more deep soil water below 6 m (Figure 8). This can be verified by our observation that soil water storage under A26 in deep

soil profiles below 6 m was significantly lower than that under A18 (Figure 2a) ($p < 0.05$). Therefore, soil water deficit was likely to be the long-term cumulative effects of root water uptake, and then changing the components of SWB. Our findings further indicated that apple trees adapt themselves to dry climate by obtaining more water through developing deeper root systems to promote fruit production, which is different from those adapting themselves to water stress through stomatal regulation.

5. Conclusions

Vegetation change has great impacts on terrestrial water cycle; however, it is challenging to decompose water balance components to explore the underlying mechanism of land use change impacts. This study aims to partition SWB under apple trees and connect it with plant water uptake strategies in the Loess Plateau. The partitioned SWB showed that the conversion of farmland to apple orchards significantly increased T and soil water deficit at the cost of decreased E and D. The changed SWB appears to be related to root water uptake since apple trees shift their water source from shallow (0–2 m) to deep soil layers (below 2 m) over the growing season, and older trees extract more water from deeper soil layer. As such, the increased T and soil water deficit were likely to be the cumulative effects of root water uptake, which subsequently changes SWB. This study provides technical support for SWB partitioning and insights into the interaction between vegetation and soil hydrological processes. Although our study indicated the relationship between SWB components and plant water uptake strategies, some aspects still requires further work to improve the understanding of ecohydrology. Specifically, the drivers of plant water use strategies have not been fully understood, which is important for the sustainability of vegetation. The SWB partitioning under different vegetations on monthly or seasonal scales is required to enhance the understanding of water cycle.

Data Availability Statement

The data used in this study are available on repository (https://doi.org/10.6084/m9.figshare.20388258.v3). The MixSIAR (version 3.1) used in this study is available at https://github.com/brianstock/MixSIAR (Stock & Semmens, 2016).

Acknowledgments
This study is jointly funded by National Natural Science Foundation of China (42071043) and Chinese Universities Scientific Fund (2452020002).

References

Allision, G. B., Gee, G. W., & Tyler, S. W. (1994). Vadose-zone techniques for estimating groundwater recharge in arid and semiarid regions. *Soil Science Society of America Journal*, *58*(1), 6–14. https://doi.org/10.2136/sssaj1994.03615995005800010002x

Al-Oqaili, F., Good, S. P., Peters, R. T., Finkenbiner, C., & Sarwar, A. (2020). Using stable water isotopes to assess the influence of irrigation structural configurations on evaporation losses in semiarid agricultural systems. *Agricultural and Forest Meteorology*, *291*, 108083. https://doi.org/10.1016/j.agrformet.2020.108083

Anderson-Teixeira, K. J., Herrmann, V., Rollinson, C. R., Gonzalez, B., Gonzalez-Akre, E. B., Pederson, N., et al. (2022). Joint effects of climate, tree size, and year on annual tree growth derived from tree-ring records of ten globally distributed forests. *Global Change Biology*, *28*(1), 245–266. https://doi.org/10.1111/gcb.15934

Baldi, P., Wolters, P. J., Komjanc, M., Viola, R., Velasco, R., & Salvi, S. (2013). Genetic and physical characterization of the locus controlling columnar habit in apple (Malus × domestica Borkh.). *Molecular Breeding*, *31*(2), 429–440. https://doi.org/10.1007/s11032-012-9800-1

Barbeta, A., Gimeno, T. E., Clavé, L., Fréjaville, B., Jones, S. P., Delvigne, C., et al. (2020). An explanation for the isotopic offset between soil and stem water in a temperate tree species. *New Phytologist*, *227*(3), 766–779. https://doi.org/10.1111/nph.16564

Barbeta, A., Jones, S. P., Clavé, L., Wingate, L., Gimeno, T. E., Fréjaville, B., et al. (2019). Unexplained hydrogen isotope offsets complicate the identification and quantification of tree water sources in a riparian forest. *Hydrology and Earth System Sciences*, *23*(4), 2129–2146. https://doi.org/10.5194/hess-23-2129-2019

Bastin, J.-F., Finegold, Y., Garcia, C., Mollicone, D., Rezende, M., Routh, D., et al. (2019). The global tree restoration potential. *Science*, *365*(6448), 76–79. https://doi.org/10.1126/science.aax0848

Benettin, P., Volkmann, T. H. M., von Freyberg, J., Frentress, J., Penna, D., Dawson, T. E., & Kirchner, J. W. (2018). Effects of climatic seasonality on the isotopic composition of evaporating soil waters. *Hydrology and Earth System Sciences*, *22*(5), 2881–2890. https://doi.org/10.5194/hess-22-2881-2018

Bowen, G. J., Putman, A., Brooks, J. R., Bowling, D. R., Oerter, E. J., & Good, S. P. (2018). Inferring the source of evaporated waters using stable H and O isotopes. *Oecologia*, *187*(4), 1025–1039. https://doi.org/10.1007/s00442-018-4192-5

Brand, W. A., Geilmann, H., Crosson, E. R., & Rella, C. W. (2009). Cavity ring-down spectroscopy versus high-temperature conversion isotope ratio mass spectrometry; a case study on δ^2H and δ^{18}O of pure water samples and alcohol/water mixtures. *Rapid Communications in Mass Spectrometry*, *23*(12), 1879–1884. https://doi.org/10.1002/rcm.4083

Brinkmann, N., Eugster, W., Buchmann, N., & Kahmen, A. (2019). Species-specific differences in water uptake depth of mature temperate trees vary with water availability in the soil. *Plant Biology*, *21*(1), 71–81. https://doi.org/10.1111/plb.12907

Bryan, B. A., Gao, L., Ye, Y., Sun, X., Connor, J. D., Crossman, N. D., et al. (2018). China's response to a national land-system sustainability emergency. *Nature*, *559*(7713), 193–204. https://doi.org/10.1038/s41586-018-0280-2

Chen, C., Park, T., Wang, X., Piao, S., Xu, B., Chaturvedi, R. K., et al. (2019). China and India lead in greening of the world through land-use management. *Nature Sustainability*, *2*, 122–129. https://doi.org/10.1038/s41893-019-0220-7

Chen, Y., Helliker, B. R., Tang, X., Li, F., Zhou, Y., & Song, X. (2020). Stem water cryogenic extraction biases estimation in deuterium isotope composition of plant source water. *Proceedings of the National Academy of Sciences of the United States of America*, *117*(52), 33345–33350. https://doi.org/10.1073/pnas.2014422117

Craig, H., & Gordon, L. I. (1965). Deuterium and oxygen 18 variations in the ocean and marine atmosphere. In E. Tongiogi (Ed.), *Stable isotopes in oceanographic studies and paleotemperatures* (pp. 9–130).

Deng, Y., Wang, S., Bai, X., Luo, G., Wu, L., Chen, F., et al. (2020). Vegetation greening intensified soil drying in some semi-arid and arid areas of the world. *Agricultural and Forest Meteorology*, *292–293*, 292–293. https://doi.org/10.1016/j.agrformet.2020.108103

Ding, Y., Nie, Y., Chen, H., Wang, K., & Querejeta, J. I. (2021). Water uptake depth is coordinated with leaf water potential, water-use efficiency and drought vulnerability in karst vegetation. *New Phytologist*, *229*(3), 1339–1353. https://doi.org/10.1111/nph.16971

Doelman, J. C., Stehfest, E., van Vuuren, D. P., Tabeau, A., Hof, A. F., Braakhekke, M. C., et al. (2020). Afforestation for climate change mitigation: Potentials, risks and trade-offs. *Global Change Biology*, *26*(3), 1576–1591. https://doi.org/10.1111/gcb.14887

Duan, H., Zhou, S., Jiang, K., Bertram, C., Harmsen, M., Kriegler, E., et al. (2021). Assessing China's efforts to pursue the 1.5°C warming limit. *Science*, *372*(6540), 378–385. https://doi.org/10.1126/science.aba8767

Evaristo, J., Jasechko, S., & McDonnell, J. J. (2015). Global separation of plant transpiration from groundwater and streamflow. *Nature*, *525*(7567), 91–94. https://doi.org/10.1038/nature14983

Feng, X., Fu, B., Piao, S., Wang, S., Ciais, P., Zeng, Z., et al. (2016). Revegetation in China's Loess Plateau is approaching sustainable water resource limits. *Nature Climate Change*, *6*(11), 1019–1022. https://doi.org/10.1038/nclimate3092

Flo, V., Martínez-Vilalta, J., Mencuccini, M., Granda, V., Anderegg, W. R. L., & Poyatos, R. (2021). Climate and functional traits jointly mediate tree water-use strategies. *New Phytologist*, *231*(2), 617–630. https://doi.org/10.1111/nph.17404

Gao, X., Zhao, X., Wu, P., Yang, M., Ye, M., Tian, L., et al. (2021). The economic–environmental trade-off of growing apple trees in the drylands of China: A conceptual framework for sustainable intensification. *Journal of Cleaner Production*, *296*, 126497. https://doi.org/10.1016/j.jclepro.2021.126497

Ge, J., Pitman, A. J., Guo, W. D., Zan, B. L., & Fu, C. B. (2020). Impact of revegetation of the Loess Plateau of China on the regional growing season water balance. *Hydrology and Earth System Sciences*, *24*(2), 515–533. https://doi.org/10.5194/hess-24-515-2020

Gessler, A., Bächli, L., Rouholahnejad Freund, E., Treydte, K., Schaub, M., Haeni, M., et al. (2021). Drought reduces water uptake in beech from the drying topsoil, but no compensatory uptake occurs from deeper soil layers. *New Phytologist*, *233*(1), 194–206. https://doi.org/10.1111/nph.17767

Gibson, J. J., & Edwards, T. W. D. (2002). Regional water balance trends and evaporation-transpiration partitioning from a stable isotope survey of lakes in northern Canada. *Global Biogeochemical Cycles*, *16*(2), 10-11–10-14. https://doi.org/10.1029/2001GB001839

Gibson, J. J., & Reid, R. (2014). Water balance along a chain of tundra lakes: A 20-year isotopic perspective. *Journal of Hydrology*, *519*, 2148–2164. https://doi.org/10.1016/j.jhydrol.2014.10.011

Good, S. P., Noone, D., & Bowen, G. (2015). Hydrologic connectivity constrains partitioning of global terrestrial water fluxes. *Science*, *349*(624), 175–177. https://doi.org/10.1126/science.aaa5931

Good, S. P., Soderberg, K., Guan, K., King, E. G., Scanlon, T. M., & Caylor, K. K. (2014). δ^2H isotopic flux partitioning of evapotranspiration over a grass field following a water pulse and subsequent dry down. *Water Resources Research*, *50*(2), 1410–1432. https://doi.org/10.1002/2013WR014333

Han, J., Tian, L., Cai, Z., Ren, W., Liu, W., Li, J., & Tai, J. (2022). Season-specific evapotranspiration partitioning using dual water isotopes in a Pinus yunnanensis ecosystem, southwest China. *Journal of Hydrology*, *608*, 127672. https://doi.org/10.1016/j.jhydrol.2022.127672

Han, Z., Huang, S., Huang, Q., Bai, Q., Leng, G., Wang, H., et al. (2020). Effects of vegetation restoration on groundwater drought in the Loess Plateau, China. *Journal of Hydrology*, *591*, 125566. https://doi.org/10.1016/j.jhydrol.2020.125566

Hermoso, V., Regos, A., Morán-Ordóñez, A., Duane, A., & Brotons, L. (2021). Tree-planting: A double-edged sword to fight climate change in an era of megafires. *Global Change Biology*, *27*(13), 3001–3003. https://doi.org/10.1111/gcb.15625

Holl, K. D., & Brancalion, P. H. S. (2020). Tree planting is not a simple solution. *Science*, *368*(6491), 580–581. https://doi.org/10.1126/science.aba8232

Huang, L. M., & Shao, M. A. (2019). Advances and perspectives on soil water research in China's Loess Plateau. *Earth-Science Reviews*, *199*, 102962. https://doi.org/10.1016/j.earscirev.2019.102962

Huang, M., & Gallichand, J. (2006). Use of the SHAW model to assess soil water recovery after apple trees in the gully region of the Loess Plateau, China. *Agricultural Water Management*, *85*(1–2), 67–76. https://doi.org/10.1016/j.agwat.2006.03.009

Huang, Y., Chang, Q., & Li, Z. (2018). Land use change impacts on the amount and quality of recharge water in the loess tablelands of China. *Science of the Total Environment*, *628–629*, 443–452. https://doi.org/10.1016/j.scitotenv.2018.02.076

Huang, Y., Evaristo, J., & Li, Z. (2019). Multiple tracers reveal different groundwater recharge mechanisms in deep loess deposits. *Geoderma*, *353*, 204–212. https://doi.org/10.1016/j.geoderma.2019.06.041

Jackson, R. B., Sperry, J. S., & Dawson, T. E. (2000). Root water uptake and transport: Using physiological processes in global predictions. *Trends in Plant Science*, *5*(11), 482–488. https://doi.org/10.1016/S1360-1385(00)01766-0

Jaramillo, F., Cory, N., Arheimer, B., Laudon, H., van der Velde, Y., Hasper, T. B., et al. (2018). Dominant effect of increasing forest biomass on evapotranspiration: Interpretations of movement in Budyko space. *Hydrology and Earth System Sciences*, *22*(1), 567–580. https://doi.org/10.5194/hess-22-567-2018

Jasechko, S., Sharp, Z. D., Gibson, J. J., Birks, S. J., Yi, Y., & Fawcett, P. J. (2013). Terrestrial water fluxes dominated by transpiration. *Nature*, *496*(7445), 347–350. https://doi.org/10.1038/nature11983

Ji, W., Huang, Y., Shi, P., & Li, Z. (2021). Recharge mechanism of deep soil water and the response to land use change in the loess deposits. *Journal of Hydrology*, *592*, 125817. https://doi.org/10.1016/j.jhydrol.2020.125817

Jia, X., Shao, M. A., Zhu, Y., & Luo, Y. (2017). Soil moisture decline due to afforestation across the Loess Plateau, China. *Journal of Hydrology*, *546*, 113–122. https://doi.org/10.1016/j.jhydrol.2017.01.011

Knighton, J., Singh, K., & Evaristo, J. (2019). Understanding catchment-scale forest root water uptake Strategies across the continental US through inverse ecohydrological modeling. *Geophysical Research Letters*, *47*(1), e2019GL085937. https://doi.org/10.1029/2019gl085937

Kool, D., Agam, N., Lazarovitch, N., Heitman, J. L., Sauer, T. J., & Ben-Gal, A. (2014). A review of approaches for evapotranspiration partitioning. *Agricultural and Forest Meteorology*, *184*, 56–70. https://doi.org/10.1016/j.agrformet.2013.09.003

Koppa, A., Alam, S., Miralles, D. G., & Gebremichael, M. (2021). Budyko-based long-term water and energy balance closure in global watersheds from Earth observations. *Water Resources Research*, *57*(5), e2020WR028658. https://doi.org/10.1029/2020WR028658

Lanning, M., Wang, L., Benson, M., Zhang, Q., & Novick, K. A. (2020). Canopy isotopic investigation reveals different water uptake dynamics of maples and oaks. *Phytochemistry*, *175*, 112389. https://doi.org/10.1016/j.phytochem.2020.112389

Li, B., Wang, Y., Hill, R. L., & Li, Z. (2019). Effects of apple orchards converted from farmlands on soil water balance in the deep loess deposits based on HYDRUS-1D model. *Agriculture, Ecosystems & Environment*, *285*, 106645. https://doi.org/10.1016/j.agee.2019.106645
Li, H., Ma, X., Lu, Y., Ren, R., Cui, B., & Si, B. (2021). Growing deep roots has opposing impacts on the transpiration of apple trees planted in subhumid loess region. *Agricultural Water Management*, *258*, 107207. https://doi.org/10.1016/j.agwat.2021.107207
Li, H., Si, B., & Li, M. (2018). Rooting depth controls potential groundwater recharge on hillslopes. *Journal of Hydrology*, *564*, 164–174. https://doi.org/10.1016/j.jhydrol.2018.07.002
Li, H., Si, B., Wu, P., & McDonnell, J. J. (2018). Water mining from the deep critical zone by apple trees growing on loess. *Hydrological Processes*, *33*(2), 320–327. https://doi.org/10.1002/hyp.13346
Li, Y., Shi, W., Aydin, A., Beroya-Eitner, M. A., & Gao, G. (2020). Loess Genesis and worldwide distribution. *Earth-Science Reviews*, *201*, 102947. https://doi.org/10.1016/j.earscirev.2019.102947
Li, Z., Chen, X., Liu, W., & Si, B. (2017). Determination of groundwater recharge mechanism in the deep loessial unsaturated zone by environmental tracers. *Science of the Total Environment*, *586*, 827–835. https://doi.org/10.1016/j.scitotenv.2017.02.061
Liu, J., Li, S., Ouyang, Z., Tam, C., & Chen, X. (2008). Ecological and socioeconomic effects of China's policies for ecosystem services. *Proceedings of the National Academy of Sciences*, *105*(28), 9477–9482. https://doi.org/10.1073/pnas.0706436105
Luo, Y., Yang, Y., Yang, D., & Zhang, S. (2020). Quantifying the impact of vegetation changes on global terrestrial runoff using the Budyko framework. *Journal of Hydrology*, *590*, 125389. https://doi.org/10.1016/j.jhydrol.2020.125389
Martín-Gómez, P., Barbeta, A., Voltas, J., Peñuelas, J., Dennis, K., Palacio, S., et al. (2015). Isotope-ratio infrared spectroscopy: A reliable tool for the investigation of plant-water sources? *New Phytologist*, *207*(3), 914–927. https://doi.org/10.1111/nph.13376
Miguez-Macho, G., & Fan, Y. (2021). Spatiotemporal origin of soil water taken up by vegetation. *Nature*, *598*(7882), 624–628. https://doi.org/10.1038/s41586-021-03958-6
Millar, C., Janzen, K., Nehemy, M. F., Koehler, G., Hervé-Fernández, P., & McDonnell, J. J. (2021). Organic contamination detection for isotopic analysis of water by laser spectroscopy. *Rapid Communications in Mass Spectrometry*, *35*(15), e9118. https://doi.org/10.1002/rcm.9118
Ning, T., Zhou, S., Chang, F., Shen, H., Li, Z., & Liu, W. (2019). Interaction of vegetation, climate and topography on evapotranspiration modelling at different time scales within the Budyko framework. *Agricultural and Forest Meteorology*, *275*, 59–68. https://doi.org/10.1016/j.agrformet.2019.05.001
Phillips, F. M. (1994). Environmental tracers for water movement in desert soils of the American southwest. *Soil Science Society of America Journal*, *58*(1), 15–24. https://doi.org/10.2136/sssaj1994.03615995005800010003x
Schlesingera, W. H., & Jasechko, S. (2014). Transpiration in the global water cycle. *Agricultural and Forest Meteorology*, *189–190*(6), 115–117. https://doi.org/10.1016/j.agrformet.2014.01.011
Schultz, N. M., Griffis, T. J., Lee, X., & Baker, J. M. (2011). Identification and correction of spectral contamination in $^{2}H/^{1}H$ and $^{18}O/^{16}O$ measured in leaf, stem, and soil water. *Rapid Communications in Mass Spectrometry*, *25*(21), 3360–3368. https://doi.org/10.1002/rcm.5236
Schwarzel, K., Zhang, L., Montanarella, L., Wang, Y., & Sun, G. (2019). How afforestation affects the water cycle in drylands: A process-based comparative analysis. *Global Change Biology*, *26*(2), 944–959. https://doi.org/10.1111/gcb.14875
Scott, D. F., & Lesch, W. (1997). Streamflow responses to afforestation with Eucalyptus grandis and Pinus patula and to felling in the Mokobulaan experimental catchments, South Africa. *Journal of Hydrology*, *199*(3), 360–377. https://doi.org/10.1016/S0022-1694(96)03336-7
Scott, R. L., Knowles, J. F., Nelson, J. A., Gentine, P., Li, X., Barron-Gafford, G., et al. (2020). Water availability impacts on evapotranspiration partitioning. *Agricultural and Forest Meteorology*, *297*, 108251. https://doi.org/10.1016/j.agrformet.2020.108251
Shao, R., Zhang, B., He, X., Su, T., Li, Y., Long, B., et al. (2021). Historical water storage changes over China's Loess Plateau. *Water Resources Research*, *57*(3), e2020WR028661. https://doi.org/10.1029/2020WR028661
Shi, P., Huang, Y., Ji, W., Xiang, W., Evaristo, J., & Li, Z. (2021). Impacts of deep-rooted fruit trees on recharge of deep soil water using stable and radioactive isotopes. *Agricultural and Forest Meteorology*, *300*, 108325. https://doi.org/10.1016/j.agrformet.2021.108325
Shi, P., Huang, Y., Yang, C., & Li, Z. (2021). Quantitative estimation of groundwater recharge in the thick loess deposits using multiple environmental tracers and methods. *Journal of Hydrology*, *603*, 126895. https://doi.org/10.1016/j.jhydrol.2021.126895
Si, B. C., & de Jong, E. (2007). Determining long-term (Decadal) deep drainage rate using multiple tracers. *Journal of Environmental Quality*, *36*(6), 1686–1694. https://doi.org/10.2134/jeq2007.0029
Sprenger, M., Leistert, H., Gimbel, K., & Weiler, M. (2016). Illuminating hydrological processes at the soil-vegetation-atmosphere interface with water stable isotopes. *Reviews of Geophysics*, *54*(3), 674–704. https://doi.org/10.1002/2015RG000515
Stock, B. C., Jackson, A. L., Ward, E. J., Parnell, A. C., Phillips, D. L., & Semmens, B. X. (2018). Analyzing mixing systems using a new generation of Bayesian tracer mixing models. *PeerJ*, *6*, e5096. https://doi.org/10.7717/peerj.5096
Stock, B. C., & Semmens, B. X. (2016). MixSIAR GUI user manual. Version 3.1 [Software]. Zenodo. https://doi.org/10.5281/zenodo.1209993
Sun, G., Zhou, G., Zhang, Z., Wei, X., McNulty, S. G., & Vose, J. M. (2006). Potential water yield reduction due to forestation across China. *Journal of Hydrology*, *328*(3), 548–558. https://doi.org/10.1016/j.jhydrol.2005.12.013
Sun, X., Wilcox, B. P., Zou, C. B., Stebler, E., West, J. B., & Wyatt, B. (2021). Isotopic partitioning of evapotranspiration in a mesic grassland during two wetting–drying episodes. *Agricultural and Forest Meteorology*, *301–302*, 108321. https://doi.org/10.1016/j.agrformet.2021.108321
Sutanto, S. J., Wenninger, J., Coenders-Gerrits, A. M. J., & Uhlenbrook, S. (2012). Partitioning of evaporation into transpiration, soil evaporation and interception: A comparison between isotope measurements and a HYDRUS-1D model. *Hydrology and Earth System Sciences*, *16*(8), 2605–2616. https://doi.org/10.5194/hess-16-2605-2012
Tao, Z., Li, H., Neil, E., & Si, B. (2021). Groundwater recharge in hillslopes on the Chinese Loess Plateau. *Journal of Hydrology: Regional Studies*, *36*, 100840. https://doi.org/10.1016/j.ejrh.2021.100840
Tao, Z., Neil, E., & Si, B. (2021). Determining deep root water uptake patterns with tree age in the Chinese loess area. *Agricultural Water Management*, *249*, 106810. https://doi.org/10.1016/j.agwat.2021.106810
Tong, X., Brandt, M., Yue, Y., Horion, S., Wang, K., Keersmaecker, W. D., et al. (2018). Increased vegetation growth and carbon stock in China karst via ecological engineering. *Nature Sustainability*, *1*(1), 44–50. https://doi.org/10.1038/s41893-017-0004-x
Vargas, A. I., Schaffer, B., Yuhong, L., & Sternberg, L. (2017). Testing plant use of mobile vs immobile soil water sources using stable isotope experiments. *New Phytologist*, *215*(2), 582–594. https://doi.org/10.1111/nph.14616
Volkmann, T. H., Haberer, K., Gessler, A., & Weiler, M. (2016). High-resolution isotope measurements resolve rapid ecohydrological dynamics at the soil-plant interface. *New Phytologist*, *210*(3), 839–849. https://doi.org/10.1111/nph.13868
Wang, C., Fu, B., Zhang, L., & Xu, Z. (2018). Soil moisture-plant interactions: An ecohydrological review. *Journal of Soils and Sediments*, *19*(1), 1–9. https://doi.org/10.1007/s11368-018-2167-0
Wang, J., Fu, B., Lu, N., Wang, S., & Zhang, L. (2019). Water use characteristics of native and exotic shrub species in the semi-arid Loess Plateau using an isotope technique. *Agriculture, Ecosystems & Environment*, *276*, 55–63. https://doi.org/10.1016/j.agee.2019.02.015

Wang, J., Fu, B., Wang, L., Lu, N., & Li, J. (2020). Water use characteristics of the common tree species in different plantation types in the Loess Plateau of China. *Agricultural and Forest Meteorology*, *288–289*, 288–289. https://doi.org/10.1016/j.agrformet.2020.108020

Wang, N., Wolf, J., & Zhang, F. S. (2016). Towards sustainable intensification of apple production in China—Yield gaps and nutrient use efficiency in apple farming systems. *Journal of Integrative Agriculture*, *15*(4), 716–725. https://doi.org/10.1016/S2095-3119(15)61099-1

Wang, Q., Cheng, L., Zhang, L., Liu, P., Qin, S., Liu, L., & Jing, Z. (2021). Quantifying the impacts of land-cover changes on global evapotranspiration based on the continuous remote sensing observations during 1982–2016. *Journal of Hydrology*, *598*, 126231. https://doi.org/10.1016/j.jhydrol.2021.126231

Wang, Y., Yan, W., Han, X., Pan, F., Cheng, L., & Liu, W. (2021). Changes in deep soil water content in the process of large-scale apple tree planting on the Loess Tableland of China. *Forests*, *12*(2), 123. https://doi.org/10.3390/f12020123

Werner, C., & Dubbert, M. (2014). Resolving rapid dynamics of soil-plant-atmosphere interactions. *New Phytologist*, *210*(3), 839–849. https://doi.org/10.1111/nph.13936

West, A. G., Goldsmith, G. R., Matimati, I., & Dawson, T. E. (2011). Spectral analysis software improves confidence in plant and soil water stable isotope analyses performed by isotope ratio infrared spectroscopy (IRIS). *Rapid Communications in Mass Spectrometry*, *25*(16), 2268–2274. https://doi.org/10.1002/rcm.5126

Wu, W., Tao, Z., Chen, G., Meng, T., Li, Y., Feng, H., et al. (2022). Phenology determines water use strategies of three economic tree species in the semi-arid Loess Plateau of China. *Agricultural and Forest Meteorology*, *312*, 108716. https://doi.org/10.1016/j.agrformet.2021.108716

Xiang, W., Evaristo, J., & Li, Z. (2020). Recharge mechanisms of deep soil water revealed by water isotopes in deep loess deposits. *Geoderma*, *369*, 114321. https://doi.org/10.1016/j.geoderma.2020.114321

Xiang, W., Si, B., Li, M., Li, H., Lu, Y., Zhao, M., & Feng, H. (2021). Stable isotopes of deep soil water retain long-term evaporation loss on China's Loess Plateau. *Science of the Total Environment*, *784*, 147153. https://doi.org/10.1016/j.scitotenv.2021.147153

Yu, K., Zhang, X., Xu, B., Li, P., Zhang, X., Li, Z., & Zhao, Y. (2021). Evaluating the impact of ecological construction measures on water balance in the Loess Plateau region of China within the Budyko framework. *Journal of Hydrology*, *601*, 126596. https://doi.org/10.1016/j.jhydrol.2021.126596

Zhang, L., Sun, P., Huettmann, F., & Liu, S. (2022). Where should China practice forestry in a warming world? *Global Change Biology*, *28*(7), 2461–2475. https://doi.org/10.1111/gcb.16065

Zhang, M., & Wei, X. (2021). Deforestation, forestation, and water supply. *Science*, *371*(6533), 990–991. https://doi.org/10.1126/science.abe7821

Zhang, S., Yang, Y., McVicar, T. R., & Yang, D. (2018). An analytical solution for the impact of vegetation changes on hydrological partitioning within the Budyko framework. *Water Resources Research*, *54*(1), 519–537. https://doi.org/10.1002/2017wr022028

Zhang, Z., Li, M., Si, B., & Feng, H. (2018). Deep rooted apple trees decrease groundwater recharge in the highland region of the Loess Plateau, China. *Science of the Total Environment*, *622–623*, 584–593. https://doi.org/10.1016/j.scitotenv.2017.11.230

Zhang, Z. Q., Evaristo, J., Li, Z., Si, B. C., & McDonnell, J. J. (2017). Tritium analysis shows apple trees may be transpiring water several decades old. *Hydrological Processes*, *31*(5), 1196–1201. https://doi.org/10.1002/hyp.11108

Zhao, L., Xiao, H., Zhou, J., Wang, L., Cheng, G., Zhou, M., et al. (2011). Detailed assessment of isotope ratio infrared spectroscopy and isotope ratio mass spectrometry for the stable isotope analysis of plant and soil waters. *Rapid Communications in Mass Spectrometry*, *25*(20), 3071–3082. https://doi.org/10.1002/rcm.5204

Zhou, S., Yu, B., Zhang, Y., Huang, Y., & Wang, G. (2016). Partitioning evapotranspiration based on the concept of underlying water use efficiency. *Water Resources Research*, *52*(2), 1160–1175. https://doi.org/10.1002/2015wr017766

Zhou, S., Yu, B., Zhang, Y., Huang, Y., & Wang, G. (2018). Water use efficiency and evapotranspiration partitioning for three typical ecosystems in the Heihe River Basin, northwestern China. *Agricultural and Forest Meteorology*, *253–254*, 261–273. https://doi.org/10.1016/j.agrformet.2018.02.002

Zhu, Y., Jia, X., & Shao, M. (2018). Loess thickness variations across the Loess Plateau of China. *Surveys in Geophysics*, *39*(4), 715–727. https://doi.org/10.1007/s10712-018-9462-6